ELSEVIER

Journal of Power Sources 63 (1996) 215–219

JOURNAL OF POWER SOURCES

Computational analysis of the gas-flow distribution in solid oxide fuel cell stacks

R.J. Boersma, N.M. Sammes *

Fuel Cell Research Group, Centre for Technology, The University of Waikato, Private Bag 3105, Hamilton, New Zealand

Received 15 August 1996; revised 13 September 1996; accepted 20 September 1996

Abstract

A computer model is developed, capable of predicting the flow distribution along the height of a fuel-cell stack. The model distinguishes a number of hydraulic resistances that are linked in series and parallel, thus forming a network to simulate the gas flow and pressure distribution in a stack. The hydraulic resistances are found from analytical solutions or from tabulated data inferred from measurements. The electrochemistry of the stack is simulated by adding or subtracting gas in the active cell area. The model is tested on an assumed separator-plate geometry and stacking height.

Keywords: Solid oxide fuel cells; Gas-flow distribution; Computational modelling; Stack

1. Introduction

Fuel cells are an exciting way of producing electricity by the electrochemical conversion of gases, such as natural gas or hydrogen, into gaseous products, waste heat and electricity. Because the reaction takes place by the electrochemical conversion of the reactants, and not via a thermal reaction, the efficiency is higher than that produced by conventional means. The efficiency can be further increased by using the waste heat in co-generation applications, see Refs. [1,2].

Solid oxide fuel cells (SOFCs) are fabricated out of all solid-state ceramic components and have many advantages over other types of fuel-cell systems, including higher temperatures for co-generation and combined heat and power (CHP) applications, all solid-state design and the possibility of using a wide range of oxidizable gases (for internal reforming processes) [3,4].

A variety of configurations has been considered for the SOFC system, including the planar, monolithic and tubular designs, although there are many other variations on these three basic designs [5].

Single cells are usually stacked into multi-cellular units, or stacks, using an interconnect or bi-polar plate. The form of the interconnect plate is dependent upon the design of the overall fuel-cell system. In the planar design, for example, the interconnect plate can be used to support the single cell, to act as a bi-polar plate, and to act as a gas manifold. The primary challenge in the design of an SOFC stack is to ensure that the interconnector performs the tasks required of it; the major design criteria is the distribution of the gases across the electrode faces [6].

It is well known that non-uniform gas distribution will have a detrimental effect on the efficiency and performance of the SOFC stack, and thus optimization of the gas-distribution profile will consequently allow for a higher power output [7].

We have shown [8] that the gas-flow distribution in a fuel-cell stack can be presented in an analytical form, assuming that the stack is viewed as a network of hydraulic resistances to the flow of gas. Using an internally-manifolded, planar stack design with an assumed geometry, the ratio between the average flow and the flow in the upper cell of the stack was determined, which could be used to ascertain separator plate design.

This paper looks at a numerical approach to the problem of non-uniform gas distribution in an internally-manifolded fuel-cell stack. The feed gases and waste gases are assumed to flow in opposite directions, which based on current technical insights is the most viable option. The numerical model is two dimensional, as it describes a cross section running through the cells, from top to bottom, including the feed and waste gas channels. The novel feature about this model is that the flow distribution is considered; most of the modelling until now has only focused on the modelling of planar or

* Corresponding author.

PII S0378-7753(96)02476-7

tubular single cells. The model is basically a numerical version of the analytical model described in Ref. [8], but it includes a larger number of resistances and their flow dependencies. The numerical approach has the advantage that a large number of physical phenomena can be included. Nevertheless, the results are difficult to verify. Therefore, the analytical approach, as presented in our previous paper [8], forms a good basis to verify the numerical results.

2. Description of the model

To calculate the flow and pressure distribution, the stack is modelled as a series and parallel connection of hydraulic resistances. Each separator plate is modelled as consisting of 12 distinguishable resistances, linked together to model the stack, as shown in Fig. 1.

The hydraulic resistances being distinguished are:

R1 Resistance to flow through the manifold channel. This is modelled as a flow through a pipe with a rough surface.

R2 Resistance attributable to the splitting of gas in the direction of the mainstream.

R3 Resistance attributable to the splitting of gas in the direction of the cell.

R4 Resistance to the flow through the gas-distribution area, which is between the actual cell and the manifold channel.

R5 Resistance caused by the contraction of the flow when entering the channels adjacent to the active area.

R6, R7 Resistance caused by the flow of the gas through the channels adjacent to the active area. The electrochemical reaction causes the gas composition to change, and thus its flow, density and viscosity change. This effect is modelled by assigning the inlet properties to the first half of the channel and the outlet properties to the second half of the channel. The outlet properties are calculated on the basis of the mass balance and the thermal balance, which follow from the current through the cell and the heat produced in the cell.

R8 Resistance caused by the expansion of the flow when leaving the channels.

R9 Resistance to the flow through the gas-collection area, which is between the actual cell and the outlet manifold channel.

R10 Resistance attributable to the addition of gas to the mainstream in the manifold channel.

R11 Resistance attributable to addition of gas in the direction of the outlet mainstream.

R12 Resistance to flow through the outlet manifold channel. This is modelled as a flow through a pipe with a rough surface.

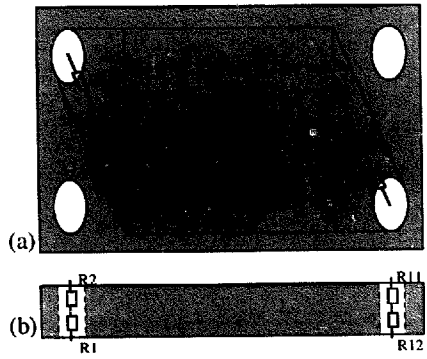

Fig. 1. The separator plate is modelled as a series and parallel linking of hydraulic resistances. The model distinguishes 12 resistances, R1 through R12, assigned to one separator plate. Plan (a) shows the separator plate from the top, with the resistances R3 through R10 projected on it. Plan (b) shows the cross section, through the manifold channels, of the plate, thus identifying the resistances R1, R2, R11 and R12.

The pressure drop across each resistance is related to the gas flow by

$$\Delta p = K \tfrac{1}{2} \rho v^2 \tag{1}$$

where K is the resistance, ρ the gas density, and v the average gas velocity. In some cases, the friction factor can be determined from formulae, in other cases it is necessary to rely on tabulated data as given in Ref. [9]. These data are likely to be measured in a certain set-up, which only matches the considered configuration to a limited extent.

The flow through the channels adjacent to the active area will be laminar in most cases. Thus, the friction factor can be given in analytical form by Eq. (2)

$$K = \frac{f}{Re} \frac{l}{D_h} \tag{2}$$

The factor f depends on the shape of the cross section of the channel [10], for a round channel $f = 64$, while for a square channel $f = 56.8$. The length of the flow path is l, Re is the Reynolds number, and D_h is the hydraulic diameter.

These formulae were used to evaluate the pressure drop across the channels (R6, R7), the resistance across the distribution area (R4), and the resistance across the collection area (R9) in the plate.

To evaluate the resistance from the divergence (R2, R3) and the convergence (R10, R11) use was made of tabulated data for ducts with a small side duct that extended from the main duct at a straight angle. Basically, the data are only valid for fully developed flow in the feeding main duct, which means that the distance between subsequent side ducts should be at least 5 to 10 main duct diameters. In the case of a fuel-cell stack, however, this distance will be only 0.1 to 0.2 diameters. This introduces some uncertainty, which can be taken away by a comprehensive analysis of this configuration,

possibly through measurements complemented with a numerical solution of the energy, impulse and mass balances.

The same holds for the contraction (R5) and the expansion (R8) before and after the channels. The flow is likely to be fully developed, but in this case the tabulated data are valid for one diameter change only, and not for a number in parallel.

The rough pipe flow (R1, R12) can be described by Eqs. (1) and (2) for low Reynolds numbers ($Re < 2300$). At higher Reynolds numbers ($Re > 3500$), the resistance becomes

$$K = \xi \frac{l}{D_h} \tag{3}$$

where ξ is the friction factor presented in, for instance, Ref. [11]. The friction factor depends on the roughness of the surface, which is defined as the ratio between the average height of the obstacles in the flow path and the pipe diameter. These data normally do not incorporate effects from splitting or combining, also care has to be taken when interpreting the results.

3. Numerical approach

The model solves pressure and flow distribution for the configurations presented in Figs. 1 and 2. Summarizing the process comes down to solving a set of equations of the form

$$\bar{p} = R_\phi \bar{\phi} \tag{4}$$

where $\bar{p}$ is a vector containing the pressure changes; $\bar{\phi}$ is a vector containing the flows; R_ϕ is a matrix containing resistance coefficients multiplied by several geometrical and physical parameters. One of these parameters is an estimate of the flow, which is identical to the flow in the elements of the flow vector ϕ, thus the problem is linearized.

The initial flow vector is found by assuming that all plates get the same flow. This produces starting values for the coefficients of the matrix, R_ϕ, and for the coefficients of the pressure vector, $\bar{p}$.

Solving the set of equations produces a new flow vector, and subsequent coefficients for the matrix and the pressure vector. This process is repeated until the difference in length of the two flow vectors, from two subsequent iterations relative to the length of the flow vector, is less than a specified value. The matrix contains $n \times 2n$ elements, where n is the number of plates. Because it is a band-matrix, with 5 bands occupied, only $5 \times 2n$ elements need to be examined.

The flow sheet of the programme is described in Fig. 3. To begin with, an input file has to be made and contain data that describes the geometry of the separator plate, the number of plates, the physical data of the gases, the gas flow and the flow added or deducted to simulate the electrochemical reactions.

To initialize the calculations, the flow is distributed evenly across the stack. From these flows, K values are determined from a formula or a table, depending on the application for each specific case. Then, the resistances that are in-line are added up, with the result that each plate now consists of four resistances, as shown in Fig. 2. As part of the linearization process, each of these resistances is multiplied by an esti-

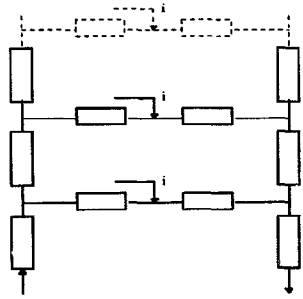

Fig. 2. The resistances per plate are added up, to give four resistances per plate. They are linked together, to simulate a network for the hydraulic resistances in a fuel-cell stack. This network gives rise to a set of equations, which after solving, gives the flow distribution in the stack.

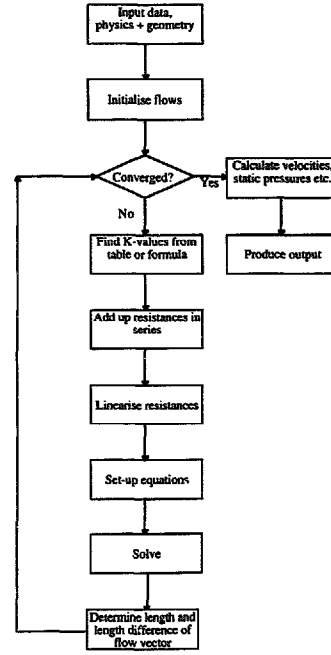

Fig. 3. Flow sheet of the model.

Table 1
Viscosity, density, composition and flow of the gases at in- and outlet of the stack. The properties at the cathode outlet differ for each load setting, but the difference with the inlet properties hardly affects the results

	Inlet anode	Outlet anode	Inlet cathode	Outlet cathode
Viscosity (Pa s)	21.7×10^{-6}	48.1×10^{-6}	46.8×10^{-6}	depends on flow and current
Density (kg/m^3)	0.022	0.21	0.31	depends on flow and current
Composition	pure H_2	20% H_2, 80% H_2O	air	depends on flow and current
Flow	set for 80% utilization	set for 80% utilization	set for $\Delta T = 150$ °C	set for $\Delta T = 150$ °C

mated value for the flow. This produces the $5\times2n$ band-matrix mentioned above. With the estimate for the flow, the pressure drop for each element can be calculated, which gives the left-hand side of Eq. (4).

The set of equations is solved with a standard routine for band-matrices, which gives the new value for the flow vector. The process of filling the resistance matrix, and the pressure vector, and the subsequent solving of the flow vector is repeated until the convergence criteria is reached.

Convergence was significantly improved by applying some under-relaxation to the flow vector; the average of the new and old flow vectors was taken as the new flow vector.

The programme was written in Turbo Pascal; the program code requires 107 kB of memory for execution and 10 kB for data. Large arrays are allocated dynamically through the use of pointers and allows data to be stored for 300 plates. The data occupy approximately 640 kB. Convergence is usually reached within seconds.

4. Case study

The analytical model that was discussed in Ref. [8] has been used to study the distribution of gas flow in the SOFC stack of Tokyo Gas [12,13]. Details of the design were not available for this study, therefore an assumed configuration was used. Because the numerical model allows for more detail than the analytical model described in Ref. [8], additional assumptions had to be made regarding the geometry of the stack, the in- and outlet gas compositions, the viscosity and the density. Table 1 shows the gases and their properties used for the calculations. The inlet data are for 850 °C, the outlet data are for 1000 °C. The cathode flow is assumed to remove all the process heat, and its flow is set accordingly. The fuel utilization is assumed to be 80% and is kept constant by adjusting the flow.

At maximum power output, the cell voltage is 0.5 V, giving 1 A cm^{-2} [13], which corresponds to 0.5 W cm^{-2}. At this setting, the heat production is at a maximum at 0.78 W cm^{-2}. For this setting, the cathode and anode gas distribution were calculated and are presented in Figs. 4 and 5, together with results for 80 and 55% of the maximum power output.

It can be concluded that the flow distribution for the cathode is most likely to be the problem, specifically at maximum power output. When the output was reduced to 80% of the maximum, however, the flow distribution was greatly improved. The flow distribution at the anode side is not likely to be a problem.

With the analytical model [8], it was calculated that for the maximum output, the ratio between the flow through the top cell and the average cell would be 0.89 for the cathode. The computer model shows that this ratio is about 0.85. This implies that the top cell gets a 15% lower flow than the average, and thus a 15% higher temperature difference.

The difference is caused mainly by the fact that the analytical model uses an average viscosity and density, whereas

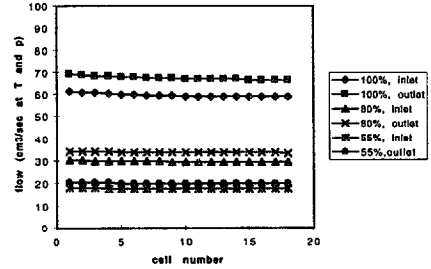

Fig. 4. Gas-flow distribution at the anode side under various loads. The flow is set for 80% utilization. The flow increase at the outlet compared with the inlet results from the density decrease, which results from the temperature increase, due to the electrochemical reactions.

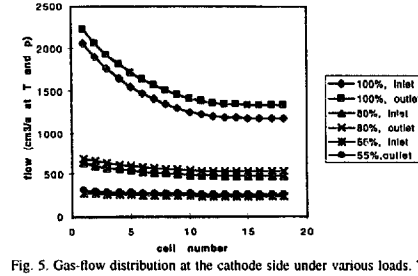

Fig. 5. Gas-flow distribution at the cathode side under various loads. The flow is set for an average temperature difference of 150 °C. The flow increase at the outlet compared with the inlet results from the density decrease, resulting from the temperature increase and the molar flow increase, resulting from the electrochemistry. The net result is an increase of the volume flow. The high flow at the lower end of the stack will effect a lower temperature difference between in- and outlet than at the high end. This will cause heat transfer from the top of the stack to the bottom.

the computer model uses different values for in- and outlet. When average values are used, the computer model and the analytical model produce practically the same results.

5. Future work

Clearly, more reliable results can be obtained by modelling the flow and heat-transfer phenomena in a dedicated computational fluid dynamics (CFD) programme, such as Fluent or Phoenics. These programmes are capable of simultaneously solving mass, impulse and energy balances for practically any configuration. They can certainly provide more accurate data on items such as splitting or combining a flow, which would add to the reliability of the model presented in this paper. Alternatively, if one is successful in combining a fuel-cell model, with a CFD code, then a very accurate stack model may be obtained. For instance, heat transfer along the height of a stack can be modelled, something which has not had much attention until now, but is justified because of the unevenness of the flow distribution that can be expected.

Also, experiments may provide data that can be correlated to numerical findings. The set-up for these experiments is not necessarily complicated, as they can be carried out at room temperature, using air as the flow medium, and built from plastic components. The inferred friction factors should also apply at high temperature and using hydrogen as a fuel.

6. Conclusions

1. A computational model was developed, describing the gas flow and pressure relationship in terms of resistances, which is numerically solved by an iterative process.

2. In the design of internally-manifolded SOFC stacks, the distribution of the cathode gas needs more attention than the distribution of the anode gas.

3. Results from the numerical and analytical model match well. This gives confidence in the reliability of both models.

References

[1] K. Foger, Conversion of natural gas to electricity in fuel cells, *Natural Gas Conversion II, Sydney, Australia, 4–9 July 1993*, p. 73.

[2] K. Aasberg-Petersen, Balance-of-plant of SOFC units for high efficiency, *1st European Solid Oxide Fuel Cell Forum, Lucerne, Switzerland, 3–7 Oct. 1994*, p. 111.

[3] T. Aida, A. Abudula, M. Ihara, H. Komiyama and K. Yamada, Direct oxidation of methane on anode of solid oxide fuel cell, *4th Int. Symp. Solid Oxide Fuel Cells, Yokohama, Japan, 18–23 June 1995*, p. 791.

[4] V. Antonucci, Natural gas reforming in small scale SOFC units, *1st European Solid Oxide Fuel Cell Forum, Lucerne, Switzerland, 3–7 Oct. 1994*, p. 183.

[5] N.Q. Minh and T. Takahashi, *Science and Technology of Ceramic Fuel Cells*, Elsevier, 1995.

[6] E. Achenbach, Ch. Bleise and J. Divisek, Modelling of Planar SOFC, *4th Int. Symp. Solid Oxide Fuel Cells, Yokohama, Japan, 18–23 June 1995*, p. 1095.

[7] A.J. Appleby and F.R. Foulkes, *Fuel Cell Handbook*, Kreiger, Malabar, FL, 1992.

[8] R.J. Boersma and N.M. Sammes, *J. Power Sources*, (1996) in press.

[9] I.E. Idel'chik, *Handbook of Hydraulic Resistance, Coefficients of local Resistance and of Friction*, US Department of Commerce, National Technical Information Service, Springfield, VA, USA.

[10] W.M. Kays and A.L. London, *Compact Heat Exchangers*, McGraw-Hill, New York, 1964.

[11] Verein Deutscher Ingenieure, *VDI Wärme-Atlas: Berechnungsblätter für den Warmeübergang*, Verein Deutscher Ingenieure, Düsseldorf, Germany, 1988.

[12] M. Hishinuma, T. Kawashima, I. Yasuda, Y. Matsuzaki and K. Ogasawara, Current Status of Planar Type SOFC Development at Tokyo Gas, *2nd European Solid Oxide Fuel Cell Forum, Oslo, Norway, 6–10 May 1996*, p. 185.

[13] M. Hishinuma, T. Kawashima, I. Yasuda, Y. Matsuzaki, K. Ogasawara and T. Ogiwara, Development of a 1 kW-Class Planar Type SOFC at Tokyo Gas, *1st European Solid Oxide Fuel Cell Forum, Lucerne, Switzerland, 3–7 Oct. 1994*, p. 953.